Contributions of Numerical Modelling to the Stability Analysis of Old Masonry Tunnels

O. Moreno Regan(✉)

Setec TPI, Paris, France
omar.moreno-regan@setec.com

Abstract. This paper presents the stability verification of an old masonry tunnel that belongs to the archaeological site of ancient Nemea, Greece. The calculations are carried out using a 2D nonlinear finite element analysis with a damage model. The study presents the results of a structural evaluation in the case that the overburden load above the tunnel increases. This tunnel was initially studied by Alexakis and Makris (2013, 2014) and solutions were provided using Limit Analysis. In this study, a comparison is given regarding the calculated bearing capacity of the tunnel between Limit Analysis and the proposed FE model. Then, several aspects of the numerical modelling of masonry tunnels are discussed. Firstly, the influence of the constitutive law of masonry and the differences between the damage model and two plastic models. Secondly, the stiffness of the surrounding ground, which has an impact on the bearing capacity of the tunnel because the earth pressure is a function of the deformation on the tunnel. And finally, the mesh size, which impacts the depth of the cracked zone and produces a variation of about 15% in the bearing capacity results. From the damage model it was found that horizontal convergences are about 3 cm before failure. This output is a major advantage of the FEM analysis with respect to limit analysis, for it allows to suggest some displacement thresholds. Lastly, a brief discussion is presented regarding the rotational capacity of the hinges as a stability verification criterion.

Keywords: Masonry · Damage · Tunnel · Vault · Underground · Nemea · Numerical uncertainty · Soil-structure interaction

1 Introduction

In the archaeological site of Ancient Nemea, Greece, south from the temple of Zeus at some 450 m, there can be found the Early Hellenistic Stadium of Nemea. The entrance to this Stadium is made through an open-air passageway that cuts into the slope of the hill on the western side of the Stadium; the passageway is followed by a 36 m vaulted masonry tunnel which remained undiscovered until 1978 (Fig. 1). This tunnel is the subject of this paper and was initially studied by Alexakis and Makris (2013, 2014) based on the findings published by Miller (2001), cited by the former. The objective of the study performed by Alexakis and Makris was to evaluate the structural stability in its current state using limit analysis, as well as an evaluation of its bearing capacity in

Y. Endo and T. Hanazato (Eds.): SAHC 2023, RILEM Bookseries 46, pp. 323–338, 2024.
https://doi.org/10.1007/978-3-031-39450-8_27

the case of an increase of the load above it; also, the objective was to shed some light regarding the exfoliation and damage observed in some stones of the tunnel. Using the preexisting results from limit analysis as a reference solution, the objective of this study is to compare and bring out some intrinsic characteristics (advantages and shortcomings) of the nonlinear FE calculations. To this end, a damage model specially conceived to study masonry is used, accompanied by other nonlinear models as a comparison. Other than the study of the bearing capacity, the objective is also to highlight the importance of the deformations of the structure near failure, which can be obtained by a FE Model. If engineering works are carried out near the tunnel, the displacements are the only thing that can be measured during the works, hence it is important to establish some thresholds on displacements to guarantee the tunnel safety. This aspect is discussed in the paper as well as the uncertainties related to FE modelling through a total of 20 models. This paper is the follow up of previous works about masonry tunnels, see Moreno Regan et al. (2017, 2018, 2022).

2 Modelling Strategy

2.1 Tunnel Description

According to Alexakis and Makris (2013, 2014) the tunnel is made up by single limestones blocks 40 cm thick, covering a span of 2.12 m; the rise of the vault is about 0.78 m and the height of the sidewalls is 1.60 m, see Fig. 1 c). There is no mortar between stone blocks, which are freely in contact with each other. The tunnel was built during the 4th century BC as a cut-and-cover tunnel, more details are presented in section Sect. 2.3.

The choice was made here to model the tunnel as a continuous medium to study the formation of hinges, the bearing capacity and the deformations, for different configurations. As a reminder, limit analysis also considers the masonry vault as an equivalent continuous medium. The soil around and under the tunnel is also modelled explicitly and the interaction between the tunnel and the soil is modelled with an interface. The calculations were made assuming plane strain conditions.

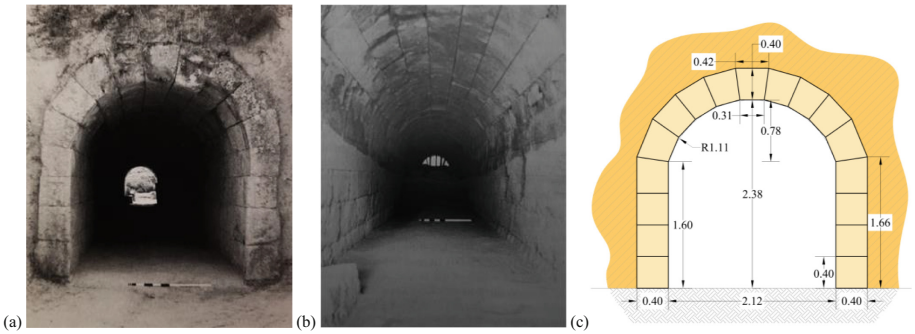

Fig. 1. Tunnel-entrance to the stadium of ancient Nemea: (a) General view of the tunnel, from the west, photo by Miller (2001), (b) Interior of the tunnel, from the East, photo by Miller (2001), (c) Tunnel dimensions (in m), according to Alexakis and Makris (2013, 2014)

2.2 Masonry

Several nonlinear models are considered for the constitutive law of the masonry. The base model is a damage model, and two plastic models are used for comparison. Their description is presented hereafter.

Damage Model. A specific model for masonry that combines homogenization and damage was developed in a previous work, Moreno Regan et al. (2017). However, the homogenization part is not considered in this study since the thickness of the tunnel is formed by a single stone block, and the homogenization is not really required. Only the isotropic damage model part is used. This model is a reworked version of the damage model by Mazars (1986), and a thorough description of the numerical model can be found in Moreno Regan et al. (2017).

This model produces a damage variable d, that reduces the elastic modulus E as the load increases:

$$\sigma_{ij} = (1 - d)C_{ijkl} : \varepsilon_{kl} \tag{1}$$

The variable d ranges from 0 to 1, with 0 corresponding to no damage. This model considers an *equivalent* strain $\widetilde{\varepsilon}$ at each Gauss point, which represents through a single variable the three-dimensional state of strain:

$$\widetilde{\varepsilon} = \gamma\sqrt{\langle\varepsilon_1\rangle_+^2 + \langle\varepsilon_2\rangle_+^2 + \langle\varepsilon_3\rangle_+^2} \text{ with } \gamma = -\frac{\sqrt{\langle\tilde{\sigma}_1\rangle_-^2 + \langle\tilde{\sigma}_2\rangle_-^2 + \langle\tilde{\sigma}_3\rangle_-^2}}{\langle\tilde{\sigma}_1\rangle_- + \langle\tilde{\sigma}_2\rangle_- + \langle\tilde{\sigma}_3\rangle_-} \tag{2}$$

where $\varepsilon_i (i = 1, 2, 3)$ are the principal strains and $\tilde{\sigma}_i$ the principal effective stress in the direction i, $\langle\varepsilon_i\rangle_+ = \varepsilon_i$ if $\varepsilon_i \geq 0$, or zero otherwise and $\langle\tilde{\sigma}_i\rangle_- = \tilde{\sigma}_i$ if $\tilde{\sigma}_i \leq 0$, or zero otherwise. The value of γ is bounded between 0 and 1 and calculated only when at least one principal effective stress is negative, i.e., in compression. At each material point, damage starts and evolves if the equivalent strain $\widetilde{\varepsilon}$ reaches an initial threshold value given by $\varepsilon_{D0} = f_t/E_0$, where f_t is the tensile strength and E_0 is the elastic modulus without damage. The expression of the damage scalar variable d is a linear combination of two variables, d_t and d_c, associated respectively with the tensile and compression stresses:

$$d = \alpha_t d_t + \alpha_c d_c \tag{3}$$

where $\alpha_t + \alpha_c = 1$. The evolution laws of the two variables of damage are:

$$d_c = 1 - \frac{\varepsilon_{D0}(1 - A_c)}{\tilde{\varepsilon}_M} - \frac{A_c}{\exp\left[B_c - (\tilde{\varepsilon}_M - \varepsilon_{D0})\right]} \tag{4}$$

$$d_t = 1 - \frac{\varepsilon_{D0}}{\tilde{\varepsilon}_M}\exp\left[-B_t(\tilde{\varepsilon}_M - \varepsilon_{D0})\right] \tag{5}$$

where A_c and B_c are parameters obtained experimentally from the stress-strain curves of a uniaxial compression test, ε_{D0} the initial threshold and $\widetilde{\varepsilon}_M$ is the actual threshold equal to ε_{D0} if it has never been reached, or the maximum value reached by $\widetilde{\varepsilon}$ otherwise.

Equation for d_t in (4), (5) includes a regularization technique in traction, to reduce mesh sensitivity problems in the finite element simulations. The parameter B_t depends on the characteristic length $l_c = \sqrt{S}$ (where S is the area of the finite element to which the integration point belongs), the mode I fracture energy G_{ft}, and the simple uniaxial tensile strength of the material σ_t according to $B_t = l_c \sigma_t / G_{\text{ft}}$.

Plastic Model 1. The first elastic-plastic model is the classic elastic perfectly plastic model with the Mohr-Coulomb criterion. The choice of the mechanical parameters c (cohesion) and φ (friction angle) are proposed in such a way as to find the following relations between compressive and tensile strength:

$$\frac{\sigma_c}{\sigma_t} = \frac{1+\sin\varphi}{1-\sin\varphi} \text{ and } \sigma_t = \frac{2c\cos\varphi}{1+\sin\varphi},\ \sigma_c = -\frac{2c\cos\varphi}{1-\sin\varphi} \tag{6}$$

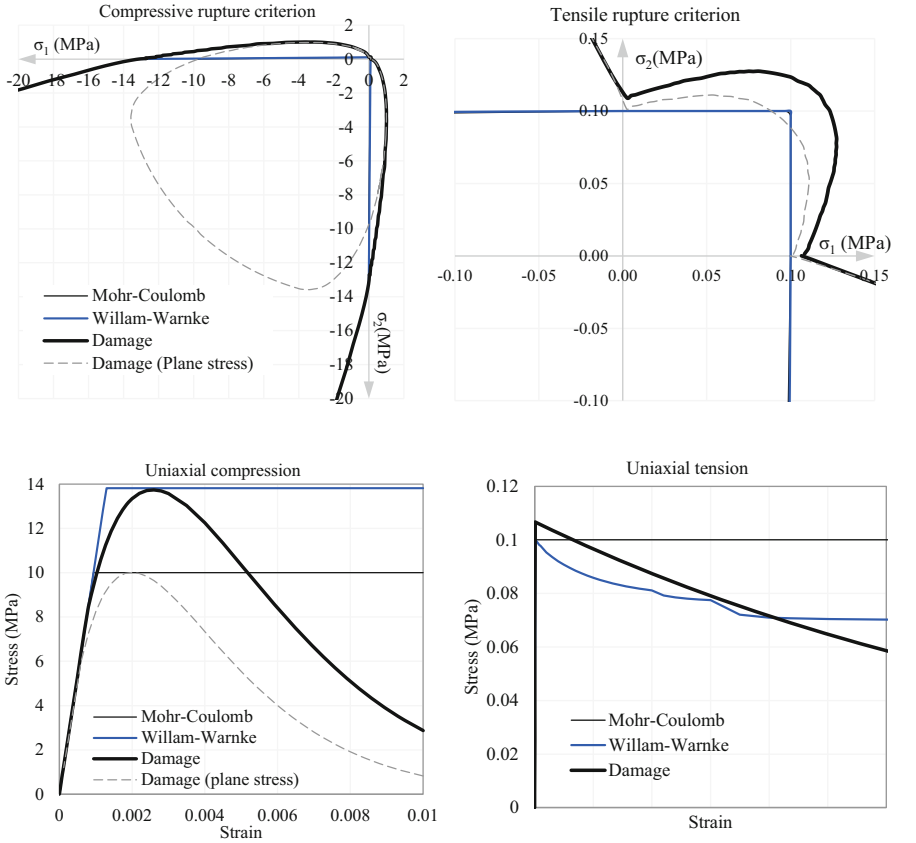

Fig. 2. Nonlinear criteria for masonry constitutive law in Plane Strain conditions ($\sigma_3 \neq 0$). With $\sigma_t = 0.1$ MPa and $\sigma_c = 10$ MPa

Plastic Model 2. The second elastic-plastic model is the 3-parameter Willam-Warnke with softening behavior in tension and perfectly plastic behavior in compression. The criterion is described in full detail by Ulm (1996).

For all three models, the criterion in the principal stress space as well as the evolution of the stress-strain relations in compression and in tension are illustrated in Fig. 2**.** It is important to notice that in plane strain conditions there is no limit in biaxial compression for any of the considered models. Properties are presented in Table 1. It was considered that the masonry has a small but no zero tensile resistance, for the sake of numerical stability. The value of $\sigma_t = 0.1$ MPa was chosen, which is consistent with values found experimentally (see Moreno Regan et al. (2018) for instance). The compressive strength $\sigma_c = 10$ MPa is the same as the one suggested by Alexakis and Makris (2013, 2014). The elastic modulus was chosen to take into account the discontinuity between blocks.

Table 1. Masonry material properties

Macnnerie			Damage model			Mohr-Coulomb			William-Warnke		
ρ	2200	kN/m^3	ε_{D0}	1.00E-05		c	0.500	MPa	σ_{bi}	10	MPa
E	10000	MPa	G_{ft}	100	Pa.m	φ	78.579		z_u	1	
ν	0.25		A_c	1.355					Z_0	0.8	
σ_t	0.1	MPa	B_c	1414					κ	1000	
σ_c	10	MPa									

2.3 Modelling Stages and Loading

According to Alexakis and Makris (2014), the tunnel was built as a cut-and-cover structure, i.e., a trench is first opened up, then the tunnel is built and finally the trench is refilled with earth. This procedure was reproduced in the model, but without considering the trench. In the first stage the tunnel is free standing over the bedrock, then a successive height of backfill of silt soil is added: 1,2,3 and 5 m; and finally, a surface load is applied (see Fig. 3). This load, distributed over the 3 m width of the tunnel, is supposed to represent a theoretical overburden added. Other possibility is to impose a displacement and then find the load by integration. The objective of the calculation is to find the maximum load (height of the overburden). The load is applied only in a 3 m width in order to have the same load case as Alexakis & Makris. Applying the load to all the width of the model would result in an increase in the horizontal load transmitted to the sidewalls and consequently, an increase in the bearing capacity of the tunnel (see Sect. 4.2), however this increase in the horizontal force was not considered by Alexakis & Makris.

In order to estimate the failure load of the masonry tunnel with the FE model, the surface load must be discretized and therefore applied by load increments. The results of the nonlinear calculations will depend on how the load is applied: applying small increments reduces the precision of the results, large increments increase it. Here, the calculation was made by discretizing the load into 50 increments. The tolerance of the nonlinear calculations was set to 0.01 and with a maximum number of iterations per

load increment of 4000. All calculations are made using CESAR-LCPC finite element software with solver rev. 062 (2021).

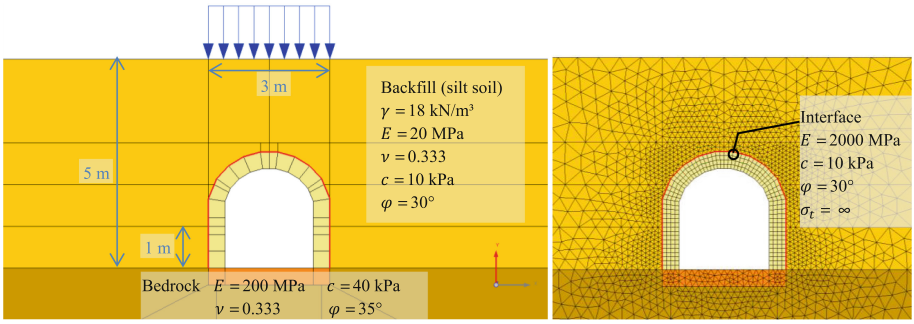

Fig. 3. Load, mesh, and properties for the FE Model

2.4 Soil and Geotechnical Considerations

The tunnel is surrounded by a backfill made of silt soil, and it stands over a formation of bedrock. The soil is modelled as an elastic perfectly plastic material using a Mohr-Coulomb criterion.

Alexakis and Makris (2014) proposed for the cohesion and friction angle of the silt Backfill, respectively, $c = 0$ kPa and $\varphi = 30°$. As it happens, with a FE model that explicitly models the soil with a surface load (see Fig. 3), it is not possible to consider a backfill with zero cohesion and at the same time search for the failure load (overburden) of the masonry vault: the soil over the vault will fail first (with a mechanism similar to Fig. 9c) before significant loads are transmitted to the masonry vault. This is why a cohesion of 10 kPa was considered for the silt backfill, and $\varphi = 30°$ as proposed by Alexakis and Makris (2014). In a similar way, the Bedrock under the sidewalls must be able to bear the vertical load coming from the tunnel sidewalls. Properties presented in Fig. 3 are proposed in such a way as to withstand an unweighted stress of 2000 kPa (see Table 2), i.e., the bearing capacity of a footing of $B = 40$ cm, using Meyerhof formula.

The choice of the elastic modulus E of the soil is a matter of interpretation, because usually the modulus of deformation needs to account for the range of strain expected in the soil next to the tunnel, as explained by Bourgeois et al. (2018). Consequently, a proper soil test should be carried out to estimate E. However, since no tests are available, we can take the plausible range of values for silt soil given, for instance, by Obrzud and Truty (2018), that goes from 2 to 40 MPa, depending on its consistency and plasticity. As a first calculation an elastic modulus of 20 MPa for the backfill is considered; for the bedrock a modulus of 200 MPa is chosen. As it will be discussed later, the value of the stiffness and shear strength properties of the soil next to the sidewalls are crucial when determining the load capacity of a masonry tunnel. The interaction between the tunnel and the surrounding ground is operated by an interface in the model. This interface allows only the sliding of the finite elements of the soil with respect to those of the tunnel. Properties are showed in Fig. 3.

3 Results: Comparison with Limit Analysis

3.1 Horizontal Earth Pressure State

The lateral earth pressure contributes greatly to the stability of the masonry vault, so its determination must be carefully established. Alexakis and Makris (2014) concluded that an active pressure state was unlikely, and therefore the most likely state was the "at rest" state, that is, the horizontal pressure is equal to $\sigma_h = K_0\sigma_v$, with $K_0 = 0.5$. To approximate this state, we have set Poisson's ratio to 0.33.

Even if the failure mechanism is different from a sliding wedge along an assumed failure plane behind a retaining wall, we assume that the active coefficient K_a can be obtained with classical approaches. The FE calculation found that the horizontal pressure at the sidewalls, before the extra overburden, lies somewhere between K_a and K_0 (Fig. 4); and this is without considering creep and consolidation phenomena that may occurred over the last 2300 years in the backfill (period of stabilization according to Miller (2001)), which can only further complexify the numerical model.

The horizontal pressure applied to the tunnel depends on its deformation, and vice versa; its estimation can only be achieved with a model that explicitly takes into account the interaction soil-structure, as will be discussed in Sect. 4.2.

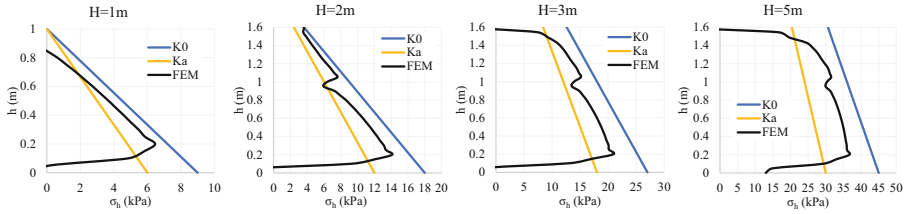

Fig. 4. Horizontal earth pressure next to the sidewall for different values of the backfill height H: Analytical vs FE Model.

3.2 Bearing Capacity of the Masonry Tunnel

Alexakis and Makris (2014) found that the tunnel in its current state has the capacity to withstand large vertical loads. When studying the additional distributed load needed to bring the tunnel to failure, they found that a load of 773 kN (per meter) was necessary, corresponding to a pressure of 258 kPa applied over the 3 m width of the tunnel (see Fig. 3), or an additional column of soil 3 m wide and 14.31 m high.

In our study the extra overburden was applied as a distributed load. The results of the damage model indicated that failure occurs for a pressure of 432 kPa. However, in the FE model this load is not entirely supported by the masonry vault alone: the soil by itself is capable of taking some of the load. Consequently, in order to find the actual load supported by the masonry vault, the axial force was investigated at the springer of the vault. Results are presented in Table 2. For the set of parameters chosen, the nonlinear FE model gives a failure load very close to limit analysis results, only 8% greater (total load

of 1006 kN vs 934 kN). Furthermore (Fig. 5) it was found that the thrust line at failure is almost identical, except at the supports, due to the chosen stiffness of the bedrock. For the calculations carried out here, the thrust line is no other that the eccentricity of the resultant force: $e = M/N$, where the axial force N and the bending moment M are obtained for each cross section normal to the mean line by integration of the normal stress. The results of the other constitutive laws and further analysis are studied in greater detail in Sect. 3.

Table 2. Load carried by the vault, initial and failure

				Limit Analysis [2]			FEM		
	Height m	Volume m^3	Weight kN/ m^3	Load kN	Each sidewall		DAM kN	PLAS 1 kN	PLAS 2 kN
					kN	kPa			
Self weight (vault)	–	1.3586	22	30	15	37	15	15	15
Initial overburden	–	7.3181	18	132	66	165	85	85	85
Failure overburden	14.31	42.93	18	773	386	966	403	141	204
Total by sidewall					467	1168	503	242	304
Total				934	934		1006	483	609
							8%	−48%	−35%

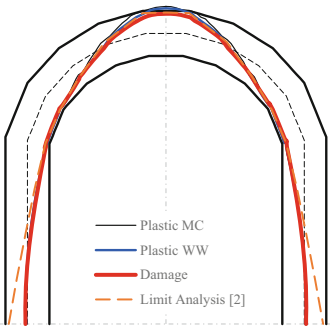

Fig. 5. Thrust lines at failure

4 Results: Advantages and Downsides of the FEM Numerical Modelling

4.1 Bearing Capacity: Compressive Strength or Hinge Mechanism?

When studying the masonry vaults of gothic churches, Heyman (1995) stated the following assumptions for masonry arches: deflections are negligible, the mean stresses are low in masonry blocks (so it is safe to assume infinite strength), and the masonry arch becomes unstable if a pattern of hinges appears which corresponds to the mechanism of collapse. In other words, failure would happen then when a hinge mechanism appears, regardless of stress. The problem is viewed as a geometrical one: a sufficient condition of stability is that the arch thickness is large enough to allow the thrust line to lie inside the masonry. However, for the case studied here, Alexakis and Makris (2014) conclude that the theoretical failure of the masonry tunnel is rather related to the increase in stress up to the compressive strength, and not to the creation of a hinge mechanism. Maximum compressive stress happens at the springer, in the intrados (Fig. 6b).

Using a FE model, the bearing capacity is reached when the calculation leads to no convergence of the iterative procedure of the solution of the nonlinear problem. However, understanding the reason of the no-convergence is another matter which demands a sometimes-extensive interpretation of the results. In our study we made sure that the no-convergence does not come from the soil failure (see Sect. 1.4), only the masonry. Using the damage model described above, we introduce now the crack related rotation through the angle θ defined by Fig. 12b. In doing so, the intent is to illustrate, if exists, the potential hinge mechanism through the rotational capacity of the hinge, i.e., the maximum angle before the no-convergence. This is clearly a result that Limit Analysis cannot provide.

Now, looking at the results obtained for different values of the compressive strength, the numerical FE model suggests that failure may be caused by the fact that the compressive strength is reached, but not in all situations. Figure 6a) shows that for all values inferior to $\sigma_c = 15$ MPa, the maximum overburden load obtained numerically increases as the compressive strength increases (in plane strain conditions, see Fig. 2). This result is similar to the conclusions by Alexakis and Makris (2014). But, for compressive strength values larger than 15 MPa, the bearing capacity of the masonry tunnel no longer increases. From Fig. 6c) we find that stresses do not continue to grow, despite the increasing strength, because the maximum rotation (rotation capacity of the hinge) appears to be limited to a value near to 35 mrad; for a value beyond this rotation, the numerical process leads to no-convergence. These results suggest that if compressive stress is large enough, the tunnel will eventually fail by a hinging mechanism.

Several modelling strategies and nonlinear constitutive laws are available in the literature for masonry structures, as comprehensively reviewed by D'Altri et al.(2020). The choice of the constitutive law and its parameters can be a source of uncertainty regarding the estimation of the bearing capacity, contrary to limit analysis, which will only require at most, the compressive strength. On the other hand, however, the prime advantage of the nonlinear FEM, as said before, is that we are able to estimate the displacements near failure, whereas limit analysis does not provide any displacements.

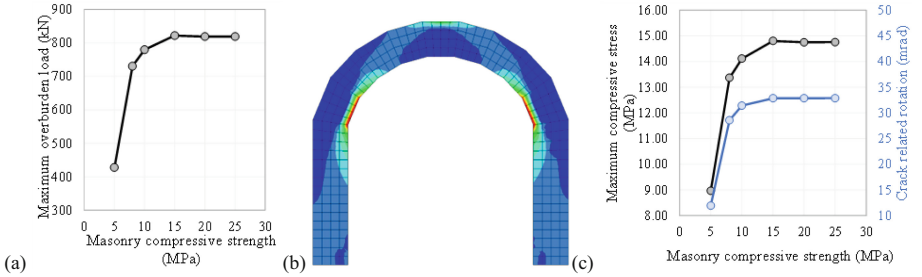

Fig. 6. Results for different compressive strengths of the masonry (Damage model only): (a) Maximum load (overburden), (b) Maximum compressive stress, (c) Maximum stress and rotation

Three different constitutive laws have been tested here, as described in section Sect. 2.2: the damage model and two plastic models.

Results are presented in Fig. 7. It was found that for this geometry and loading scenarios, only the damage model is capable to produce significant displacements (horizontal convergences larger than 10 mm), and to reach greater loads. Plastic models remain conservative when estimating the bearing capacity (Table 2). The shortcomings of an elastic calculation for the masonry have been discussed in Moreno Regan et al. (2022). The evolution of the maximum compressive stress is similar in all models, except the elastic model which underestimates it (Fig. 7b); however only the damage model makes it possible to reach values close to the compressive strength of 14 MPa (see Fig. 2). In Fig. 7c) it can be seen that, when the numerical failure occurs, the damage model produces a greater rotation at the hinge; and a horizontal convergence of about 3 cm; and about 1 cm for the Plastic model. This order of magnitude of the deformations have been observed in practice, see Moreno Regan et al. (2022).

If an overburden were actually to take place near the tunnel, the structure will be monitored to measure its deformation, hence the importance of knowing the displacements thresholds, rather than the maximum load, that may indicate if we are near failure or not. The thresholds illustrated is Fig. 7a) could, for instance, be proposed in order to oversee the works and ensure its safety. The "attention threshold" could be placed around 2–3 mm of horizontal convergence, close to the beginning of the nonlinear behavior (whatever the constitutive law), and it could be synonym of extra measures to be taken in the work site; whereas the "warning threshold" could be placed near 20 mm to indicate that we are approaching failure and that the works must be stopped, and reinforcements placed.

Figure 8 shows the strain concentration near the cracks for all the constitutive laws. It can clearly be seen that the Mohr-Coulomb criterion will only produce a plastic zone (sometimes large) which does not correspond to any physical crack. Only the damage and the Willam-Warnke models (with strain softening in tension) will produce an accurate strain concentration that represents the crack. Consequently, it can be concluded that the damage model, and to a lesser extent, the Willam-Warnke model, can be expected to predict more accurately the real displacements and deformations of the vault.

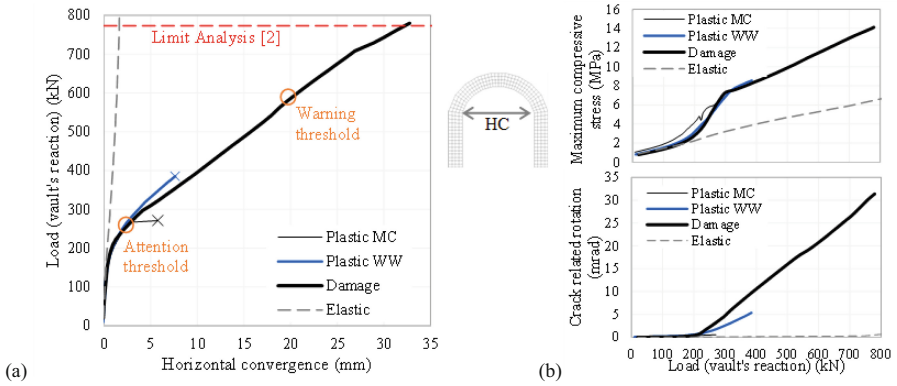

Fig. 7. Results for different models / constitutive laws: (a) Load-convergence (positive convergence means an increase of the distance between sidewalls), (b) Maximum stress and rotation

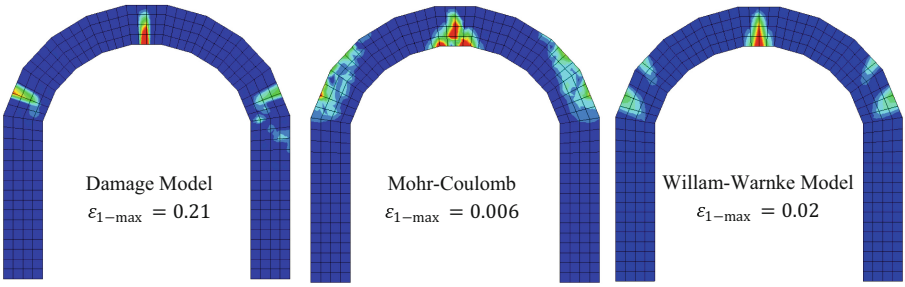

Fig. 8. Masonry principal total strain ε_1 (tension) for different models

4.2 Impact of the Soil Properties

The stiffness and shear strength properties of the soil next to the sidewalls have an important influence on the stability of the tunnel, see Moreno Regan et al. (2022). Six models were built to study the influence of the stiffness of the backfill. The pressures transmitted to the tunnel are a result of the deformation of the structure, and vice versa.

From an initial value of the horizontal pressure due to the weight of 5 m of soil (Fig. 4), the pressure increases inexorably with the increasing surface load, in proportion to the stiffness of the ground, contrary to the hypothesis by Alexakis and Makris (2014) who preserve a constant value. The horizontal pressure transmitted to the sidewalls, see Fig. 9 a), increases with stiffer soil, because a more rigid ground will provide a higher lateral reaction. On the contrary, soft soil will allow the deformation of the tunnel providing less lateral reaction, even no reaction at all for a modulus of 5 GPa, until 200 kN of load. The consequence is that the tunnel will have a smaller bearing capacity, since the supports of the vault can move more freely. With a soft ground (5 MPa) the bearing capacity is around 400 kN, whereas for a stiff ground (50 MPa) the bearing capacity is near 700 kN, almost the double.

In Fig. 9 b) it can be seen that, if the ground modulus is less than 20 MPa, the maximum compressive stress is less than the compressive strength (about 14 MPa), and failure occurs because of the creation of a hinge mechanism: again, the maximum crack related rotation reaches a value close to 35 mrad (see §0) before the no-convergence of the model. If the ground is stiff enough, the deformations will be constrained, and numerical failure occurs when the compressive strength is reached, see Fig. 9 b), in our case for elastic modulus superior to 20 MPa.

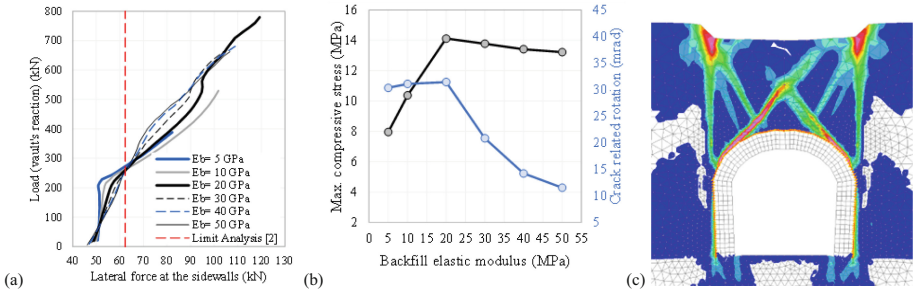

Fig. 9. Impact of the soil properties (damage model): (a) Resultant lateral force for different stiffness of the Backfill, (b) Results for different Backfill modulus, (c) Soil plastic strain at masonry failure (Eb = 20 MPa)

4.3 Mesh Sensitivity and Crack Depth

It is known that a damage model with strain softening (see Fig. 2) has dependency issues regarding the mesh size, making it necessary to use a regularization technique to mitigate the problem. This was done in our damage model as explained in Sect. 2.2. In a more general way, it is worth noting that the solution produced by a finite element model will always depends, to some extent, on the mesh size, whatever the constitutive law used in the nonlinear domain. Three different meshes were tested here (see Fig. 10) with the three constitutive laws discussed above to illustrate the range of results that can be found and try to give an estimate, however approximate may be, of the uncertainty related to the mesh size.

Results are presented in Fig. 11. As it can be seen in Fig. 11e) the depth of the crack depends on the size of the mesh. The smaller the mesh, the smaller the compressed area in the cracked cross section, producing a higher compressive stress, and this regardless of the constitutive law. For the damage model, we have found a relative standard deviation (RSD) of the maximum compressive stress of 43%, and 30% and 28% for the plastic models, respectively. Regarding the bearing capacity of the masonry tunnel, the RSD is about 14% for the damage model and 16% and 11% for the Plastic models, respectively (Fig. 11a). As it can be seen the uncertainty is greater regarding the maximum compressive stresses.

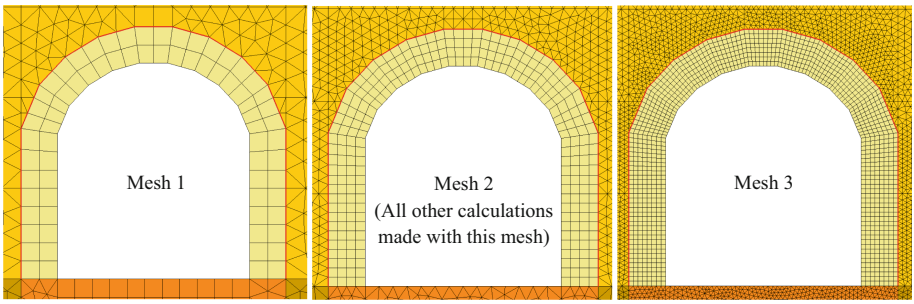

Fig. 10. Different mesh sizes tested in the calculations

Strain-stress relation evolve differently with each mesh. On the other hand, displacements seem to be less uncertain than stresses: in Fig. 11c) we see that for the damage model, meshes 2 and 3 present very similar load-convergence curves (only the coarse mesh gives a different result) contrary to maximum stresses in Fig. 11b). Also, the RSD of the crack related rotation (Fig. 11d) is 23% for the damage model; 45% and 46% for the plastic models.

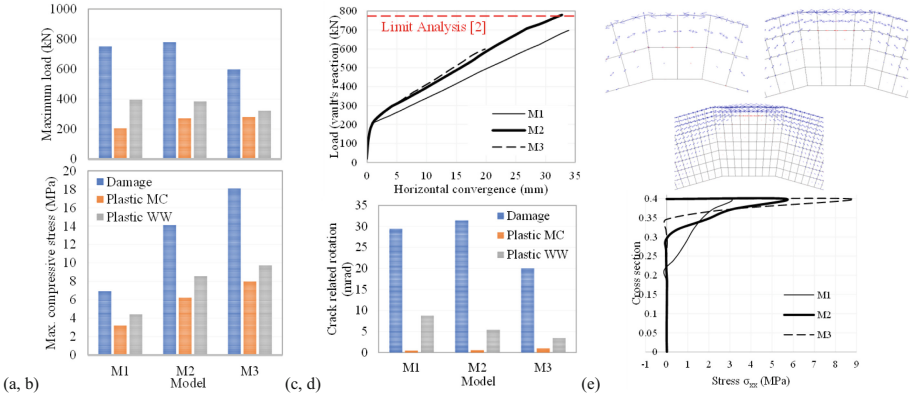

Fig. 11. Impact of the size of mesh for the FE Model: (a, b, c, d) Results for different mesh sizes, (e) Principal stress vectors at the crown

5 Rotational Capacity

When the stability of an existing masonry tunnel must be verified, usually we verify that the calculated stress and internal forces remain under certain limits, see Moreno Regan et al. (2022), even though the compressive strength is implicitly verified if the model converges. It was found here that a certain value of rotation of the hinge is never exceeded in the calculations, a value close to 35 mrad (around 2 °). It means that from this type of calculation some safe limit can be established *a priori* (Fig. 12b); then, the rotational capacity of the hinges could be checked as a stability verification.

The idea of the limitation of the rotation of the hinge is actually not new: it is already a verification demanded by Eurocode 2 (§5.6.3) for cracked reinforced concrete structures when a plastic calculation is made. However, for masonry structures there is no limitation in design codes regarding displacements or rotations; although in a recent addition to Eurocode 6 (masonry structures) it is prescribed that the maximum strain of masonry in uniaxial compression should not exceed 2.0‰ (that we used here, see in Fig. 2 the uniaxial compression curve marked "Damage plane stress").

It appears then that such verification can be used to verify the stability of an existing tunnel, in complement (or sometimes instead) of stress verification which can be uncertain, depending on the properties of the numerical model; displacements been less uncertain in their evolution (see Fig. 12a). This idea will be explored in further research.

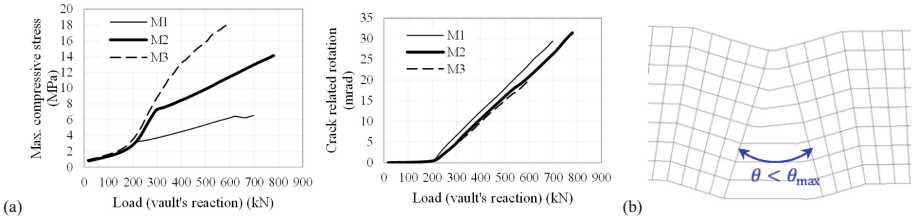

(a) (b)

Fig. 12. Study of the crack related rotation at the crown: (a) Influence of the mesh on the maximal values of stress and rotation, (b) Maximum crack related rotation

6 Conclusions

The bearing capacity of an existing tunnel can be assessed using a FE nonlinear model and results can be close to those produced by limit analysis. In this study, the ancient masonry tunnel in Nemea was analyzed. With the initial set of assumptions, the calculation showed a bearing capacity of 1006 kN vs 934 kN estimated with limit analysis [1, 2]. For this geometry and load scenario, failure of the masonry tunnel occurs when the compressive strength is reached. Nonetheless, beyond a certain compressive strength and for soft ground around the tunnel, the failure mechanism obtained numerically is rather a hinge mechanism. The apparition of a hinge mechanisms can be interpreted in a FE model when a crack related rotation reaches a certain limit. Our calculations gave a limit close to 35 mrad. It can be suggested to introduce a hinge rotation verification as a complement or instead of a stress check, when assessing the bearing capacity of a masonry vault. This idea will be explored in further research.

Also, it is worth point out the fact that a FE model allows to estimate the displacement near failure, which makes it possible to propose threshold values to oversee the works: an "attention threshold" of 2–3 mm and a "warning threshold" of 20 mm, for the horizontal convergence tunnel.

The FEM assessment comes however with some uncertainties, related to the constitutive law and to the parameters for the masonry and soil. On the other hand, we also have the uncertainties of numerical nature, like the mesh size, the discretization of the load, the parameters of the nonlinear algorithm with its maximum number of iterations, the chosen precision, among others. Here, some of these were tested.

Firstly, the constitutive law of the masonry. When modelling quasi-brittle materials like masonry it appears to be more adequate to use a constitutive law with softening behavior, because perfectly plastic behavior may not properly estimate strain concentration (cracks), and thus stresses and deformations. The damage model gives a good estimation regarding the expected strain concentration and deformations of the tunnel. The plastic Willam-Warnke model gives more conservative results regarding maximum compressive stress but follows the same pattern as the damage model. Elastic models will completely underestimate the maximal values of stress and deformations and should be avoided.

Secondly, the load and the ground around the tunnel. The pressure applied to the tunnel depends on its deformation, and vice versa. A more rigid ground provides a higher lateral reaction increasing the bearing capacity. A soft soil allows the deformation of the tunnel causing earlier failure through a hinge mechanism. An increase from 5 MPa (unlikely) to 50 MPa in the elastic modulus of the backfill can almost double the bearing capacity. In general, this problem can be treated through a parametric study within a plausible range of values. Also, it should be noted that the no-convergence of the calculation could happen because of soil failure rather than masonry failure, and thus an interpretation of the results is needed.

Finally, the mesh size. It was observed that the bearing capacity may present a variation of about 15% and the maximum compressive stress of about 40%. Coarse meshes should be avoided when modeling cracks, since, as it was seen, the crack depth is limited to the size of the elements and if only 2 elements are used, the crack will be limited numerically to half the cross section, which it will not correspond to the physical reality; also, it should be noted that a very refined mesh size can considerably increase the calculation time. As a good measure, at least 10 integration points should be placed in the cross section. In general, the opinion of the author is that results coming from a FE model should be penalized.

References

Alexakis, H., Makris, N.: Stability analysis of the underground masonry tunnel of ancient Nemea. In: Bilotta, E., Flora, A., Lirer, S., Viggiani, C. (eds.) Geotechnical Engineering for the Preservation of Monuments and Historic Sites 2013, pp. 113–21. CRC Press (2013). https://doi.org/10.1201/b14895

Alexakis, H., Makris, N.: Structural stability and bearing capacity analysis of the tunnel-entrance to the stadium of Ancient Nemea. Int. J. Archit. Heritage **7**(6), 673–692 (2014). https://doi.org/10.1080/15583058.2012.662262

Bourgeois, E., Burlon, S., Cuira, F.: Modélisation numérique des ouvrages géotechniques. Techniques de l'ingénieur, Mécanique des sols et géotechnique (2018). https://doi.org/10.51257/a-v1-c258

D'Altri, A.M., et al.: Modeling strategies for the computational analysis of unreinforced masonry structures: review and classification. Arch. Comput. Methods Eng. **27**(4), 1153–1185 (2019). https://doi.org/10.1007/s11831-019-09351-x

Heyman, J.: The stone skeleton. Structural engineering of masonry architecture. Cambridge University Press, 1st edn, Cambridge, UK (1995)

Mazars, J.: A description of micro- and macroscale damage of concrete structures. Eng. Fract. Mech. **25**, 729–737 (1986). https://doi.org/10.1016/0013-7944(86)90036-6

Miller, S.G.: Excavations at Nemea II. The early Hellenistic Stadium. University of California Press, Berkley and Los Angeles, USA (2001)

Moreno Regan, O., Bourgeois, E., Colas, A.S., Chatellier, P., Desbordes, A., Douroux, J.F.: Application of a coupled homogenization-damage model to masonry tunnel vaults. Comput. Geotechnics **83**, 132–141 (2017) https://doi.org/10.1016/j.compgeo.2016.10.024

Moreno Regan, O., Bourgeois, E., Colas, A.S., Chatellier, P., Desbordes, A., Douroux, J.F.: Experimental characterization of the constitutive materials composing an old masonry vaulted tunnel of the Paris subway system. Int. J. Archit. Heritage **12**(2), 195–215 (2018). https://doi.org/10.1080/15583058.2017.1388883

Moreno Regan, O., Bourgeois, E., Douroux, J.F.: On the stability of underground masonry vaults: the case of the mairie d'ivry station of the Paris Metro. Int. J. Archit. Heritage 1–22 (2022). https://doi.org/10.1080/15583058.2022.2108354

Obrzud, R., Truty, A.: The hardening Soil Model – A practical Guidebook. Z_Soil. PC 100707 (2018). report revised 21 Oct 2018

Ulm, F.J.: Un modèle d'endommagement plastique : application aux bétons de structure. Études et Recherches des laboratoires des ponts et chaussées. Série Ouvrages d'Art OA19. LCPC (1996)